Real-time Green's Functions based on the Non-Crossing Approximation

Hristiana Atanasova

February 25, 2018

Contents

1 Introduction

2 Models

2.1 Hubbard Model

2.2 Anderson Impurity Model

A general impurity Hamiltonian has the form

$$\mathrm{H_{imp}} = \mathrm{H_D} + \mathrm{H_B} + \mathrm{H_{hyb}}. \tag{1}$$

We consider the single-orbital Anderson impurity model (AIM) with the following dot-Hamiltonian

$$\mathrm{H_D} = \sum_{\sigma\epsilon\uparrow,\downarrow} \varepsilon_\sigma \mathrm{d}_\sigma^\dagger \mathrm{d}_\sigma + \mathrm{U}\mathrm{d}_\uparrow^\dagger \mathrm{d}_\uparrow \mathrm{d}_\downarrow^\dagger \mathrm{d}_\downarrow,$$

ε_σ are the on-site energy levels and U is the interaction between electrons having opposite spins. $\mathrm{H_{imp}}$ can in general incorporate a time-dependence, but for now we will consider only time-independent impurity models. There are four possible dot eigenstates $|0\rangle, |\uparrow\rangle, |\downarrow\rangle, |\uparrow\downarrow\rangle$ corresponding to the dot being empty or occupied by either one or two electrons. The non-interacting bath Hamiltonian has the form

$$\mathrm{H_B} = \sum_{\sigma,\lambda} \varepsilon_\lambda \mathrm{b}_\lambda^\dagger \mathrm{b}_\lambda$$

and the coupling between dot and bath is given through the Hybridization

$$\mathrm{H_{hyb}} = \sum_{\sigma,\lambda} (\mathrm{t}_{\sigma\lambda} \mathrm{b}_\lambda^\dagger \mathrm{d}_\sigma + \mathrm{t}_{\sigma\lambda}^* \mathrm{d}_\sigma^\dagger \mathrm{b}_\lambda),$$

which describes processes in which electrons are hopping from the bath to the dot and vice versa.

A general procedure to evaluate expectation values $\langle \cdots \rangle$ is to split $\mathrm{H_{imp}}$ into a sum $\mathrm{H_{imp}} = \mathrm{H_0} + \mathrm{H_{int}}$. The time propagation can be calculated exactly in $\mathrm{H_0}$ while $\mathrm{H_{int}}$ is treated by pertubation expansion. For a weak electron-coupling (small U) one expands in terms of the paramter U and the rest of the Hamiltonian is treated axactly. When one is dealing with strong electron correlations (large U) $\mathrm{H_D}$ and $\mathrm{H_B}$ sum up to $\mathrm{H_0}$ and the expansion is performed in terms of $\mathrm{H_{hyb}}$. The latter is called the strong coupling approach.

3 Methods

3.1 Dynamical mean field theory for systems in equilibrium

Dynamical Mean Field Theory is a method to solve a lattice problem with many degrees of freedom by mapping it to an impurity problem consisting of a single correlated site embedded in an uncorrelated bath. The bath is formed by the residual sites of the lattice and the hybridization between the impurity and the bath (the dynamical mean field) is the function $\Delta(\omega)$. It resembles the exchange of particles with the rest of

the lattice and must be determined self consistently as a functional of the lattice Greens function $G(\omega)$. The key approximation in DMFT is the local nature of the lattice self energy

$$\Sigma_{ij}^{lat}(\omega) \backsimeq \delta_{ij}\Sigma^{imp}(\omega)$$

that justifies the mapping.

In equilibrium all functions depend only on time-differences and can be expressed by their Fourier transforms. For time-dependent systems (e.g. an electric-field-driven lattice system) they become two-times objects and incorporate the overall temporal evolution of the system as well as quantum fluctuations. In the following the DMFT equations for systems in equilibrium will be presented and an extension to time-dependend systems follows later. The simplest model for the description of strongly correlated systems is the single band Hubbard model representing a collection of single orbital atoms placed at the nodes of a crystal lattice

$$H_{Hub} = -\sum_{\langle i,j\rangle,\sigma} \widetilde{v}_{ij} d_{i\sigma}^{\dagger} d_{j\sigma} + \sum_{i} U(d_{i\uparrow}^{\dagger} d_{i\uparrow} - \frac{1}{2})(d_{i\downarrow}^{\dagger} d_{i\downarrow} - \frac{1}{2}).$$

The operators $d_{i\uparrow}^{\dagger}[d_{i\uparrow}]$ create[destroy] an electron with spin σ in an Wannier orbital at a crystal site i, $\widetilde{v}_{ij}$ is the hopping between neighbouring sites, which depends on the overlap of neighbouring orbitals and U is the local Coulomb interaction between electrons. The hopping matrix element must be scaled properly with the coordination number Z, so that it remains finite in the limit of $lim_{Z\to\infty}(\widetilde{v}\sqrt{Z} = v)$. With the approximation that the lattice self energy is local in space one is able to compute the local Greens function $G_{ii}^{\sigma}(t - t') = -i\langle \mathcal{T} d_{i\sigma}(t) d_{i\sigma}^{\dagger}(t')\rangle$ from an effective impurity model described by the following action

$$S = i\int_{c} dt U n_{\uparrow}(t) n_{\downarrow}(t) - i\sum_{\sigma}\int_{c} dt dt' d_{\sigma}^{\dagger}(t) \triangle(t - t') d_{\sigma}(t').$$

From here on the spin index will be supressed for simplicity. The impurity self energy is defined via the Dyson equation

$$G_{ii}^{-1}(\omega) = \omega + \mu - \triangle(\omega) - \Sigma^{imp}(\omega)$$

and will be used to obtain the lattice Greens function

$$G_{ij}^{-1}(\omega) = \delta_{ij}[\omega + \mu - \Sigma_{ii}(\omega)] - v_{ij}.$$

In real space this means that all non-local components of the lattice self energy $\Sigma_{ij}(\omega)$ are neglected and the local component is approximated by $\Sigma^{imp}(\omega)$. For a translationally invariant system ($\Sigma_{ii}(\omega) \equiv \Sigma(\omega)$) one averages over the whole Brillouin zone to get the on-site component of the lattice Green function, which is referred to as the self-consistency condition

$$G_{ii}(\omega) = \frac{1}{L}\sum_{k} G_{k}(\omega) = \frac{1}{L}\sum_{k} \frac{1}{\omega + \mu + \Sigma(\omega) - \epsilon_{k}},$$

with $G_k(\omega)$ the momentum resolved Greens function, L the number of lattice sites and ϵ_k the dispersion relation of the non-interacting tight binding band

$$\epsilon_{k} = \sum_{j} v_{ij} exp^{ik(R_i - R_j)}.$$

Instead of performing the k-summation one can integrate over the local, non-interacting Density of states $\mathrm{D}(\epsilon) = \frac{1}{\mathrm{L}} \sum_{\mathrm{k}} \delta(\epsilon - \epsilon_{\mathrm{k}})$

$$\mathrm{G_{ii}}(\omega) = \int \frac{\mathrm{D}(\epsilon)}{\omega + \mu + \Sigma(\omega) - \epsilon_{\mathrm{k}}}.$$

The self-consistency condition relates for each frequency ω the dynamical mean field to the local Green's function. This functional relation G[Δ] provides a closed set of equations to determine Δ and G. This can be done by an iterative procedure that does not depend on the initial guess for Δ.

3.2 Systems out of equilibrium

To capture non-equilibirum physics one must extend the dynamical mean field $\Delta(\omega)$ to a time-dependent field $\Delta(t, t')$. In the limit $d \to \infty$ the self energy is local in space

$$\Sigma_{ij}(t, t') = \delta_{ij} \Sigma_i(t, t')$$

and is used to obtain the contour-ordered lattice Green's function $\mathrm{G_{ij}(t, t')} = -\mathrm{i}\langle \mathcal{T} \mathrm{d_i(t) d_j^\dagger(t')} \rangle$ from a Dyson equation

$$G_{ij}^{-1}(t, t') = (G_0^{-1})_{ij}(t, t') - \delta_{ij} \Sigma_{ii}(t, t')$$

with the non-interacting lattice Green's function $(G_0^{-1})_{ij}(t, t')$. Like in the equilibrium case one has to solve the effective impurity action

$$\mathrm{S} = \mathrm{i} \int_{\mathrm{c}} \mathrm{dt U n_\uparrow(t) n_\downarrow(t)} - \mathrm{i} \sum_\sigma \int_{\mathrm{c}} \mathrm{dt dt' d_\sigma^\dagger(t) \triangle(t, t') d_\sigma(t')},$$

where $\Sigma(t, t')$ is implicitly defined via the Dyson equation of the impurity system. The set of equations for non-equilibirum DMFT is formally identical to the one for equilibrium DMFT with the crucial difference that all objects depend on two times. In the Dyson equation for $G_{ij}(t, t')$ the self energy plays the role of a memory kernel.

3.3 Time-dependent electric fields

Within non-equilibrium DMFT many physical problems, like the application of electromagnetic driving fields, can be treated. A time-dependent electromagnetic field converts the hopping term $v_{ij}(t)$ into

$$v_{ij}(t) = v_{ij} \exp\left(-\frac{ie}{\hbar} \int_{\vec{R}_i}^{\vec{R}_j} d\vec{r} \vec{A}(\vec{r}, t) \right),$$

where the vector potential $\vec{A}(\vec{r}, t)$ is treated as a phase factor and a scalar potential term $e \sum_{i\sigma} \Phi(\vec{R}_i, t) d_{i\sigma}^\dagger d_{i\sigma}$ is added to the Hamiltonian. This corresponds to a Pierls substitution, which is derived from the requirement that the Hamiltonian is gauge-invariant. With a time-dependent hopping the self-consistency condition for a semi-circular Density of States generalizes from $\Delta(t, t') = v_0^2 G(t, t')$ to

$$\Delta(t, t') = v(t) G(t, t') v^*(t').$$

Applying an unpolarized AC electric field propagating in the z-direction results in a time-periodic linear potential originating from the root of the Bethe lattice via a driving term

$$H_{drv}(t) = \sum_j eaE_0 sin(\omega t) s_j n_j,$$

with the electric charge e, the amplitude of the field E_0, the angular frequency of the driving ω and s_j the number of steps from the root of the tree to site j. Performing the unitary transformation

$$U(t) = \exp\left[i\phi(t) \sum_j s_j n_j \right],$$

where $\phi(t) = -(eaE_0/\omega)cos(\omega t)$, the full Hamiltonian $H(t) = H_{Hub} + H_{drv}(t)$ can be transformed into the rotating-frame Hamiltonian

$$H_{rot}(t) = i\frac{dU(t)}{dt}U^\dagger(t) + U(t)H(t)U^\dagger(t)$$

$$= -i\sum_l eaE_0 sin(\omega t) s_l n_l \exp\left[i\phi(t)\sum_l s_l n_l \right] \exp\left[-i\phi(t)\sum_k s_k n_k \right] +$$

$$\exp\left[i\phi(t)\sum_l s_l n_l \right] \left[-\sum_{\langle i,j\rangle,\sigma} v_{ij} d^\dagger_{i\sigma} d_{j\sigma} + \sum_i U(d^\dagger_{i\uparrow}d_{i\uparrow} - \frac{1}{2})(d^\dagger_{i\downarrow}d_{i\downarrow} - \frac{1}{2}) + \sum_i eaE_0 sin(\omega t) s_i n_i \right] \exp\left[-i\phi(t)\sum_k s_k n_k \right]$$

$$= -\sum_l eaE_0 sin(\omega t) s_l n_l \exp\left[\phi(t)\sum_l s_l n_l \right] \exp\left[i\phi(t)\sum_k s_k n_k \right] +$$

$$\exp\left[i\phi(t)\sum_l s_l n_l \right] i\sum_l eaE_0 sin(\omega t) s_l n_l \exp\left[i\phi(t)\sum_k s_k n_k \right] +$$

$$(1 + i\phi(t)\sum_l s_l n_l + ...) \times -\sum_{\langle i,j\rangle,\sigma} v_{ij} d^\dagger_{i\sigma} d_{j\sigma} \times -(1 + i\phi(t)\sum_k s_k n_k + ...) +$$

$$(1 + i\phi(t)\sum_l s_l n_l + ...) \times -\sum_i U(d^\dagger_{i\uparrow}d_{i\uparrow} - \frac{1}{2})(d^\dagger_{i\downarrow}d_{i\downarrow} - \frac{1}{2}) \times -(1 + i\phi(t)\sum_k s_k n_k + ...) +$$

$$= eaE_0 sin(\omega t) s_k \times \exp\left[\phi(t)\sum_l s_l n_l \right] \exp\left[i\phi(t)\sum_k s_k n_k \right] \times \sum_{l\neq k} eaE_0 sin(\omega t) s_l n_l \times (1 - 1) +$$

$$\exp\left[-i\phi(t)s_k\right] \exp\left[i\phi(t)s_l\right] \times -\sum_{\langle i,j\rangle,\sigma} v_{ij} d^\dagger_{i\sigma} d_{j\sigma} \times \exp\left[i\phi(t)\sum_{k\neq i,j} s_k n_k \right] \exp\left[-i\phi(t)\sum_{l\neq i,j} s_l n_l \right] +$$

$$\exp\left[-i\phi(t)s_i\right] \exp\left[i\phi(t)s_i\right] \times -\sum_i U(d^\dagger_{i\uparrow}d_{i\uparrow} - \frac{1}{2})(d^\dagger_{i\downarrow}d_{i\downarrow} - \frac{1}{2}) \times \exp\left[i\phi(t)\sum_{k\neq i} s_k n_k \right] \exp\left[-i\phi(t)\sum_{l\neq i} s_l n_l \right]$$

This results in the elimination of the driving term. The rotating frame Hamiltonian H_{rot} and H_{Hub} differ only by a time-dependent Pierls phase on the hopping amplitude

$$v_{ij}(t) = v_{ij} \exp^{iA(s_i - s_j)cos(\omega t)} .$$

The factor (s_i - s_j)=$\pm$1 implies nearest neighbor hopping and we define the dimensionless driving amplitude as $A = eaE_0/\omega$.

3.4 Open systems

Real materials can exchange energy and particles with their environment, which should be included into the description of our system. Continuously driving an open system with an external field enables the energy injected into the system to dissipate into the bath and the emergence of a steady state.

One can describe dissipation of energy to other degrees of freedom by coupling every site of the lattice to an environment. In DMFT two dissipation mechanisms have been adopted so far. The first one couples each lattice site to a reservoir of non-interacting fermions. The free-fermion bath has the same structure as the bath in the Anderson impurity model and is defined by

$$\mathrm{H_f} = \mathrm{H_{fBath}} + \mathrm{H_{fmix}} \tag{2}$$

$$\mathrm{H_{fBath}} = \sum_{\mathrm{k},\sigma} \varepsilon_{\mathrm{k}} \mathrm{f}^{\dagger}_{\mathrm{k},\sigma} \mathrm{f}_{\mathrm{k},\sigma}$$

and

$$\mathrm{H_{fmix}} = \sum_{\mathrm{k},\sigma} (\mathrm{V_k} \mathrm{f}^{\dagger}_{\mathrm{k},\sigma} \mathrm{d}_{\sigma} + \mathrm{V}^{*}_{\mathrm{k}} \mathrm{d}^{\dagger}_{\sigma} \mathrm{f}_{\mathrm{k},\sigma}),$$

where $d^{\dagger}_{\sigma}(d_{\sigma})$ creates (annihilates) an electron on the dot, $f^{\dagger}_{k}(f_k)$ creates (annihilates) a bath degree of freedom, ε_k describes the bath energy levels and V_k is the hybridization between the bath modes and the impurity. The bath is in thermal equilibrium with a defined tamperature T and a chemical potential μ_k, which is chosen such that there is no current flow between the bath and the impurity. Since the bath has a bilinear structure it can be integrated out analytically and it turns out that it contributes to the system through an additional self-energy correction. The Dyson equation can be symbolically written as

$$G(t,t') = (G_0^{-1}(t,t') - \Sigma_{fBath}(t,t') - \Sigma(t,t'))^{-1}, \tag{3}$$

where all objects are matrices and the bath self-energy is given by

$$\Sigma^{\alpha\alpha}_{fBath}(t,t') = \sum_{\beta} G^{\beta\beta}(t,t') \times \Lambda^{\alpha\alpha}_{\beta}(t,t')$$

with the bath hybridization function $\Lambda^{\alpha\alpha}_{\beta}(t,t')$ defined via the coupling densities $\Gamma(\omega) = \pi \sum_k V_k V_k^* \delta(\omega + \mu_k - \epsilon_{k,\sigma})$ and the initial occupation given by the Fermi-Dirac distribution like in 4. The simplest treatment of the dissipation is to chose Γ to be a flat density of states with a soft cutoff $\Gamma(\omega) = \frac{\lambda}{(1+\exp^{\nu(\omega-\omega_c)})(1+\exp^{-\nu(\omega+\omega_c)})}$ ($\nu = \omega_c = 10$ and $\lambda = \Gamma(0)$).

The second dissipation mechanism is the coupling to a bosonic bath, which can be described via the Holstein coupling with the local phonon bath Hamiltonian

$$H_{phBath} = \sum_q \omega_q b_q^\dagger b_q.$$

Here $b_q^\dagger(b_q)$ are creation (annihilation) operators and ω_q is the frequency of the phonon mode q. The electron-phonon coupling is given by

$$H_{phMix} = \sum_q \lambda_q (b_q^\dagger + b_q)(n_d - 1),$$

where n_d is the total dot occupation and λ_d the coupling strength between the dot and the phonon modes. The factor -1 has no physical meaning, but is there to sustain particle-hole symmetry for the energy level $\epsilon = 0$. The properties of the bath are fully defined by the spectral function $J(\omega) = \pi \sum_q \frac{\lambda_q^2}{\omega_q} \delta(\omega - \omega_q)$. We assume that the coupling to the phonon bath is weak and perform second order pertubation theory. Similar to 3 the Dyson equation takes the form

$$G(t,t') = (G_0^{-1}(t,t') - \Sigma_{phBath}(t,t') - \Sigma(t,t'))^{-1},$$

but here the phonon self-energies do not change the state of the dot:

$$\Sigma_{phBath}^{\alpha\alpha}(t,t') = G^{\alpha\alpha}(t,t') \times \Lambda^{\alpha\alpha}(t,t').$$

The phonon Hybridization function is defined by

$$\Lambda^{\alpha\alpha}(t,t') = <\alpha|(n_d(t)-1)(n_d(t')-1)|\alpha> \times \sum_q \lambda_q^2 Tr_b[\rho_b((b_q^\dagger(t) + b_q(t'))(b_q^\dagger(t) + b_q(t'))]$$

and if we consider that the bath is composed of free harmonic phonon modes we can write it as $\Lambda^{\alpha\alpha}(t-t') = (n_d^{(\alpha)} - \delta)^2 \times \Lambda_b(t-t')$, where

$$\Lambda_b(t-t') = \sum_q \lambda_q^2 B_q(t-t').$$

As for the fermion bath, the spectral function $J(\omega) = \frac{2}{\pi}\sum_q (\lambda_q^2/\omega_q)\delta(\omega - \omega_q)$ describes the properties of the phonon bath and $\Lambda_b(t-t')$ becomes

$$\Lambda_b(t-t') = \frac{2}{\pi}\int d\omega J(\omega)\omega B_\omega(t-t').$$

We chose a Lorentzian shape for the spectral function $J(\omega) = \frac{1}{\pi\gamma\left[1+\left(\frac{\omega-\omega_0}{\gamma}\right)^2\right]}$ with $\gamma = 0.5$ and $\omega_0 = 1$.

3.5 Solving the impurity problem

3.5.1 Bold propagators

We are interested in the calculation of correlation functions/Green's functions like $\mathrm{G}^{>}(\mathrm{t},\mathrm{t}') = -\mathrm{i}\langle \mathrm{d}(\mathrm{t})\mathrm{d}^\dagger(\mathrm{t}')\rangle$ and $\mathrm{G}^{<}(\mathrm{t},\mathrm{t}') = \mathrm{i}\langle \mathrm{d}^\dagger(\mathrm{t}')\mathrm{d}(\mathrm{t})\rangle$ from which we can obtain information about the system, like the spectral function $\mathrm{A}(\omega)$, in certain regimes. The spectral functions represents the density of single particle excitations at energy ω. The times $\mathrm{t}_1, \mathrm{t}_2$ exist on the real part of the Keldysh contour. In the strong coupling approach we assume that the interaction between electrons is strong and the coupling to the bath infinitesimally weak, so we

expand in terms of the hybridization H_{hyb}. The expectation value $\langle \cdots \rangle$ of an operator O at time t is given by

$$\langle O(t) \rangle = \mathrm{Tr}\left(\rho U^{\dagger}(t)\hat{O}U(t)\right),$$

with the initial density matrix ρ, that can be factorized into the dot ρ_D and the bath ρ_B density matirx, since the dot is initially decoupled from the bath. In the interaction picture the operators, here denoted by a hat $\widehat{\ }$, have the time dependency

$$\hat{O}(t) = \exp^{iH_0 t} O \exp^{-iH_0 t},$$

with the reduced Hamiltonian$H_0 = H_{imp} - H_{hyb}$ containing information about the coupling U. The interaction picture time evolution propagator is given by

$$U(t) = \exp^{iH_0 t} \exp^{-iHt}.$$

$U(t)$ $\left[U^{\dagger}(t)\right]$can be though of the propagation on the upper [lower] branch of the Keldysh contour obeying the differential equation

$$\frac{\partial}{\partial t}U(t) = i \exp^{iH_0 t}(H_0 - H)\exp^{-iH_0 t}$$
$$= -i \exp^{iH_0 t} H_{hyb}(\exp^{-iH_0 t}\exp^{iH_0 t})\exp^{iHt}$$

$$= -i\widehat{H}_{hyb}(t)U(t).$$

After integrating both sides with respect to time

$$U(t) = 1 - i\int_0^t dt_1 \widehat{H}_{hyb}(t_1)U(t_1)$$

and after repeatedly iterating we arrive at

$$U(t) = \sum_{n=0}^{\infty}(-i)^n \int_0^t dt_1 \int_0^{t_1} dt_2 \cdots \int_0^{t_{n-1}} dt_n \widehat{H}_{hyb}(t_1)\widehat{H}_{hyb}(t_2)\cdots\widehat{H}_{hyb}(t_n)$$

with time ordering $t_1 \succ t_2 \succ \ldots \succ t_n$. The Hybridization term in the interaction picture can be written in the following form

$$\widehat{H}_{hyb}(t) = \exp^{iH_0 t} V \exp^{-iH_0 t}$$

$$= \sum_{n=0}^{\infty}\frac{i}{n!}^n (H_0 t)^n \sum_{\sigma,\lambda}(t_{\sigma\lambda}b_{\sigma}^{\dagger}d_{\sigma} + t_{\sigma\lambda}^{\star}d_{\sigma}^{\dagger}b_{\lambda})\sum_{n=0}^{\infty}\frac{(-i)}{n!}^n (H_0 t)^n$$

$$= \sum_{\sigma,\lambda}\sum_{n=0}^{\infty}\frac{i}{n!}^n (\varepsilon_{\sigma}d_{\sigma}^{\dagger}d_{\sigma} + Un_{\uparrow}n_{\downarrow} + \varepsilon_{\lambda}b_{\lambda}^{\dagger}b_{\lambda})^n (t)^n \sum_{\sigma,\lambda}(t_{\sigma\lambda}b_{\sigma}^{\dagger}d_{\sigma} + t_{\sigma\lambda}^{\star}d_{\sigma}^{\dagger}b_{\lambda})\sum_{n=0}^{\infty}\frac{(-i)}{n!}^n (\varepsilon_{\sigma}d_{\sigma}^{\dagger}d_{\sigma} + Un_{\uparrow}n_{\downarrow} + \varepsilon_{\lambda}b_{\lambda}^{\dagger}b_{\lambda})^n (t)^n$$

Using $[d_{\sigma}, n_{\uparrow}n_{\downarrow}] = d_{\bar{\sigma}}$ and Baker-Hausdorff theorem

$$\mathrm{d}_\sigma(\mathrm{t}) = \exp^{\mathrm{iH_0 t}} \mathrm{d}_\sigma \exp^{-\mathrm{iH_0 t}} = \exp^{-\mathrm{itL_{H_0}}} \mathrm{d}_\sigma,$$

where $L_{H_0} d_\sigma \equiv [d_\sigma, H_0] = \sum_{\sigma\epsilon\uparrow,\downarrow} \varepsilon_\sigma \left[d_\sigma, d_\sigma^\dagger d_\sigma\right] = \sum_{\sigma\epsilon\uparrow,\downarrow} \varepsilon_\sigma d_\sigma$, we arrive at

$$\widehat{\mathrm{H}}_{\mathrm{hyb}}(\mathrm{t}) = \sum_{\sigma,\lambda} \left\{ \mathrm{t}_{\sigma\lambda} \exp^{\mathrm{i}(\varepsilon_\sigma + \mathrm{U d}_\sigma^\dagger \mathrm{d}_\sigma - \varepsilon_{\sigma\lambda})\mathrm{t}} \mathrm{b}_{\sigma\lambda}^\dagger \mathrm{d}_\sigma + \mathrm{t}_{\sigma\lambda}^\star \exp^{-\mathrm{i}(\varepsilon_\sigma + \mathrm{U d}_\sigma^\dagger \mathrm{d}_\sigma - \varepsilon_{\sigma\lambda})\mathrm{t}} \mathrm{d}_\sigma^\dagger \mathrm{b}_{\sigma\lambda} \right\}$$

The first step is to compute so called bold propagators $\mathrm{G}_{\alpha\beta}(\mathrm{t})$ between many body states α and β containing all hybridization lines that do not cross each other in a given time intervall. The hybridization lines exist only on one branch and do not connects times between the two branches. Propagators on the upper and lower branch obey the relation$\mathrm{G}_{\alpha\beta}^\dagger(\mathrm{t}) = \mathrm{G}_{\alpha\beta}(\bar{\mathrm{t}})$. We start with the formal expression

$$\mathrm{G}_{\alpha\beta}(\mathrm{t}) = \langle\langle \alpha \mid \rho_{\mathrm{D}} \exp^{-\mathrm{iHt}} \mid \beta \rangle\rangle_{\mathrm{B}} = \langle\langle \alpha \mid \rho_{\mathrm{D}} \exp^{-\mathrm{iH_0 t}} \mathrm{U}(\mathrm{t}) \mid \beta \rangle\rangle_{\mathrm{B}},$$

where $\langle \cdots \rangle_{\mathrm{B}} = \mathrm{Tr}\{\rho_{\mathrm{B}} \cdots\}$denotes that the bath degrees are traced out. We insert the expansion for U

$$\mathrm{G}_{\alpha\alpha}(\mathrm{t}) = \langle\langle \alpha \mid \rho_{\mathrm{D}} \exp^{-\mathrm{iH_0 t}} \mid \alpha \rangle\rangle_{\mathrm{B}} + (-\mathrm{i})^2 \int_0^{\mathrm{t}} \mathrm{dt}_1 \int_0^{\mathrm{t}_1} \mathrm{dt}_2 \langle\langle \alpha \mid \rho_{\mathrm{D}} \exp^{-\mathrm{iH_0 t}} \widehat{\mathrm{H}}_{\mathrm{hyb}}(\mathrm{t}_1) \widehat{\mathrm{H}}_{\mathrm{hyb}}(\mathrm{t}_2) \mid \alpha \rangle\rangle_{\mathrm{B}} + \cdots$$

$$= \sum_\beta \langle\langle \alpha \mid \beta \rangle\langle \beta \mid \exp^{-\mathrm{iH_0 t}} \mid \alpha \rangle\rangle_{\mathrm{B}} - \sum_\beta \sum_{\sigma,\lambda} \int \mathrm{dt}_1 \int_0^{\mathrm{t}_1} \mathrm{dt}_2 \left|\mathrm{t}_{\sigma\lambda}\right|^2 \times$$
$$\left(\langle\langle \alpha \mid \exp^{-\mathrm{iH_0 t}} \mathrm{d}_\sigma \mid \beta \rangle\langle \beta \mid \mathrm{d}_\sigma^\dagger \hat{\mathrm{b}}_{\sigma\lambda}^\dagger(\mathrm{t}_1) \hat{\mathrm{b}}_{\sigma\lambda}(\mathrm{t}_2) \mid \alpha \rangle\rangle_{\mathrm{B}} + \langle\langle \alpha \mid \exp^{-\mathrm{iH_0 t}} \mathrm{d}_\sigma^\dagger \mid \beta \rangle\langle \beta \mid \mathrm{d}_\sigma \hat{\mathrm{b}}_{\sigma\lambda}(\mathrm{t}_2) \hat{\mathrm{b}}_{\sigma\lambda}^\dagger(\mathrm{t}_1) \mid \alpha \rangle\rangle_{\mathrm{B}} \right) + \cdots$$

$$= \delta_{\alpha\beta} \exp^{-\mathrm{i}\varepsilon_\alpha \mathrm{t}} - \sum_\beta \int_0^{\mathrm{t}} \mathrm{dt}_1 \int_0^{\mathrm{t}_1} \mathrm{dt}_2 \mathrm{G}_{\alpha\alpha}^{(0)}(\mathrm{t} - \mathrm{t}_1) \mathrm{G}_{\beta\beta}^{(0)}(\mathrm{t}_1 - \mathrm{t}_2) \times$$
$$\left(\langle \alpha \mid \mathrm{d}_\sigma \mid \beta \rangle\langle \beta \mid \mathrm{d}_\sigma^\dagger \mid \alpha \rangle \sum_{\sigma,\lambda} \left|\mathrm{t}_{\sigma\lambda}\right|^2 \langle \hat{\mathrm{b}}_{\sigma\lambda}^\dagger(\mathrm{t}_1) \hat{\mathrm{b}}_{\sigma\lambda}(\mathrm{t}_2) \rangle_{\mathrm{B}} + \langle \alpha \mid \mathrm{d}_\sigma^\dagger \mid \beta \rangle\langle \beta \mid \mathrm{d}_\sigma \mid \alpha \rangle \sum_{\sigma,\lambda} \left|\mathrm{t}_{\sigma\lambda}\right|^2 \langle \hat{\mathrm{b}}_{\sigma\lambda}(\mathrm{t}_2) \hat{\mathrm{b}}_{\sigma\lambda}^\dagger(\mathrm{t}_1) \rangle_{\mathrm{B}} \right) \mathrm{G}_{\alpha\alpha}(\mathrm{t}_2) + \cdots$$

$$= \mathrm{G}_{\alpha\alpha}^{(0)}(\mathrm{t}) - \sum_\beta \int_0^{\mathrm{t}} \mathrm{dt}_1 \int_0^{\mathrm{t}_1} \mathrm{dt}_2 \mathrm{G}_{\alpha\alpha}^{(0)}(\mathrm{t} - \mathrm{t}_1) G_{\beta\beta}^{(0)}(t_1 - t_2) \times$$
$$\left(\langle \alpha \mid \mathrm{d}_\sigma \mid \beta \rangle\langle \beta \mid \mathrm{d}_\sigma^\dagger \mid \alpha \rangle \triangle_\sigma^< (\mathrm{t}_1 - \mathrm{t}_2) + \langle \alpha \mid \mathrm{d}_\sigma^\dagger \mid \beta \rangle\langle \beta \mid \mathrm{d}_\sigma \mid \alpha \rangle \triangle_\sigma^> (\mathrm{t}_1 - \mathrm{t}_2) \right) \mathrm{G}_{\alpha\alpha}^{(0)}(\mathrm{t}_2) + \cdots$$

with the bare atomic state propagators $\mathrm{G}_{\alpha\alpha}^{(0)}(\mathrm{t}) = \exp^{-\mathrm{i}\varepsilon_\alpha \mathrm{t}}$ leaving the dot state invariant. Note that both the bare $\mathrm{G}_{\alpha\alpha}^{(0)}(\mathrm{t})$ and bold propagator $\mathrm{G}_{\alpha\alpha}(\mathrm{t})$ are diagonal for the Anderson impurity model because the trace over the bath degrees gives results only for an even number of creation and annhilation operators. Therefore only square terms of $\widehat{\mathrm{H}}_{\mathrm{hyb}}$ appear in the expansion for G. In DMFT the hybridization function $\triangle_\sigma^{>/<}$ is obtained from the self-consistency condition. Here we will write it in terms of the coupling density

$\Gamma(\omega) = \pi \sum_k \mid t_k \mid^2 \delta(\omega - \varepsilon_k)$ that fully describe the bath and hybridization and the initial Fermi Dirac distribution $f(\omega - \mu) = \frac{1}{1+\exp^{\beta(\omega-\mu)}}$

$$\triangle^<(\mathrm{t}_1, \mathrm{t}_2) = \int_{-\infty}^{\infty} \frac{\mathrm{d}\omega}{\pi} \exp^{-\mathrm{i}\omega(\mathrm{t}_1 - \mathrm{t}_2)} \mathit{\Gamma}(\omega) \mathrm{f}(\omega - \mu) \tag{4}$$

and

$$\triangle^>(\mathrm{t}_1, \mathrm{t}_2) = \int_{-\infty}^{\infty} \frac{\mathrm{d}\omega}{\pi} \exp^{-\mathrm{i}\omega(\mathrm{t}_1 - \mathrm{t}_2)} \mathit{\Gamma}(\omega)(1 - \mathrm{f}(\omega - \mu)).$$

With the approximation for the self-energy, that it includes only hybridizaton lines that do not cross, the Dyson equation can be written as

$$\mathrm{G}_{\alpha\alpha}(\mathrm{t}) = \mathrm{G}^{(0)}_{\alpha\alpha}(\mathrm{t}) - \int_0^{\mathrm{t}} \mathrm{dt}_1 \int_0^{\mathrm{t}_1} \mathrm{dt}_2 \mathrm{G}^{(0)}_{\alpha\alpha}(\mathrm{t} - \mathrm{t}_1) \mathit{\Sigma}_{\alpha\alpha}(\mathrm{t}_1 - \mathrm{t}_2) \mathrm{G}_{\alpha\alpha}(\mathrm{t}_2)$$

with

$$\mathit{\Sigma}_{\alpha\alpha}(t_1 - t_2) = \sum_\sigma \sum_\beta G_{\beta\beta}(t_1 - t_2) \times \\ \big(\langle \alpha \mid \mathrm{d}_\sigma \mid \beta \rangle \langle \beta \mid \mathrm{d}^\dagger_\sigma \mid \alpha \rangle \triangle^<_\sigma (\mathrm{t}_1 - \mathrm{t}_2) + \langle \alpha \mid \mathrm{d}^\dagger_\sigma \mid \beta \rangle \langle \beta \mid \mathrm{d}_\sigma \mid \alpha \rangle \triangle^>_\sigma (\mathrm{t}_1 - \mathrm{t}_2) \big).$$

For the four different initial states (denoted by the outer index α) on the dot we can derive a set of coupled Dyson equations

$$\mathrm{G}_0(\mathrm{t}) = \mathrm{G}^{(0)}_0(\mathrm{t}) - \int_0^{\mathrm{t}} \mathrm{dt}_1 \int_0^{\mathrm{t}_1} \mathrm{dt}_2 \mathrm{G}^{(0)}_0(\mathrm{t} - \mathrm{t}_1) \mathrm{G}_\uparrow(\mathrm{t}_1 - \mathrm{t}_2) \Delta^<_\uparrow(\mathrm{t}_1 - \mathrm{t}_2) \mathrm{G}_0(\mathrm{t}_2) - \\ \int_0^{\mathrm{t}} \mathrm{dt}_1 \int_0^{\mathrm{t}_1} \mathrm{dt}_2 \mathrm{G}^{(0)}_0(\mathrm{t} - \mathrm{t}_1) \mathrm{G}_\downarrow(\mathrm{t}_1 - \mathrm{t}_2) \Delta^<_\downarrow(\mathrm{t}_1 - \mathrm{t}_2) \mathrm{G}_0(\mathrm{t}_2)$$

$$\mathrm{G}_\uparrow(\mathrm{t}) = \mathrm{G}^{(0)}_\uparrow(\mathrm{t}) - \int_0^{\mathrm{t}} \mathrm{dt}_1 \int_0^{\mathrm{t}_1} \mathrm{dt}_2 \mathrm{G}^{(0)}_\uparrow(\mathrm{t} - \mathrm{t}_1) \mathrm{G}_0(\mathrm{t}_1 - \mathrm{t}_2) \Delta^>_\uparrow(\mathrm{t}_1 - \mathrm{t}_2) \mathrm{G}_\uparrow(\mathrm{t}_2) - \\ \int_0^{\mathrm{t}} \mathrm{dt}_1 \int_0^{\mathrm{t}_1} \mathrm{dt}_2 \mathrm{G}^{(0)}_\uparrow(\mathrm{t} - \mathrm{t}_1) \mathrm{G}_{\uparrow\downarrow}(\mathrm{t}_1 - \mathrm{t}_2) \Delta^<_\downarrow(\mathrm{t}_1 - \mathrm{t}_2) \mathrm{G}_\uparrow(\mathrm{t}_2)$$

$$\mathrm{G}_\downarrow(\mathrm{t}) = \mathrm{G}^{(0)}_\downarrow(\mathrm{t}) - \int_0^{\mathrm{t}} \mathrm{dt}_1 \int_0^{\mathrm{t}_1} \mathrm{dt}_2 \mathrm{G}^{(0)}_\downarrow(\mathrm{t} - \mathrm{t}_1) \mathrm{G}_0(\mathrm{t}_1 - \mathrm{t}_2) \Delta^>_\uparrow(\mathrm{t}_1 - \mathrm{t}_2) \mathrm{G}_\downarrow(\mathrm{t}_2) - \\ \int_0^{\mathrm{t}} \mathrm{dt}_1 \int_0^{\mathrm{t}_1} \mathrm{dt}_2 \mathrm{G}^{(0)}_\downarrow(\mathrm{t} - \mathrm{t}_1) \mathrm{G}_{\uparrow\downarrow}(\mathrm{t}_1 - \mathrm{t}_2) \Delta^<_\downarrow(\mathrm{t}_1 - \mathrm{t}_2) \mathrm{G}_\downarrow(\mathrm{t}_2)$$

$$\mathrm{G}_{\uparrow\downarrow}(\mathrm{t}) = \mathrm{G}^{(0)}_{\uparrow\downarrow}(\mathrm{t}) - \int_0^{\mathrm{t}} \mathrm{dt}_1 \int_0^{\mathrm{t}_1} \mathrm{dt}_2 \mathrm{G}^{(0)}_{\uparrow\downarrow}(\mathrm{t} - \mathrm{t}_1) \mathrm{G}_\downarrow(\mathrm{t}_1 - \mathrm{t}_2) \Delta^>_\uparrow(\mathrm{t}_1 - \mathrm{t}_2) \mathrm{G}_{\uparrow\downarrow}(\mathrm{t}_2) - \\ \int_0^{\mathrm{t}} \mathrm{dt}_1 \int_0^{\mathrm{t}_1} \mathrm{dt}_2 \mathrm{G}^{(0)}_{\uparrow\downarrow}(\mathrm{t} - \mathrm{t}_1) \mathrm{G}_\uparrow(\mathrm{t}_1 - \mathrm{t}_2) \Delta^>_\downarrow(\mathrm{t}_1 - \mathrm{t}_2) \mathrm{G}_{\uparrow\downarrow}(\mathrm{t}_2),$$

which can be solved by a self consistent iteration. All entities depend only on time differences and one can evaluate the integrals in the Fourier space, where convolutions become simple multiplications. Before starting with the first iteration, the bold propagators $G_{\alpha\alpha}(t)$ are initialized by the bare propagators $G^{(0)}_{\alpha\alpha}(t)$ from which the first self-energy is obtained. Both are inserted into the Dyson equation with the interaction times integrated over. With the updated $G_{\alpha\alpha}(t)$ one can go back to the second step and compute a new self energy for the next iteration cycle until convergence is reached.

3.5.2 Correlation functions

So far we have calculated propagators between many body states, which contain all non-crossing hybridization lines in a time segment on a single branch. These objects have no physical meaning, to calculate physical observables it is necessary to include hybridization lines connecting times on both branches. We introduce so called vertex functions $K_{\alpha\beta}(t,t')$ with the first[second] time index on the upper[lower] branch. A vertex funcion incorporates all non-crossing intra- and inter-branch hybrdization lines. The procedure to estimate $K_{\alpha\beta}(t,t')$ is similar to the calculation of $G_{\alpha\alpha}(t)$ with the difference that $K_{\alpha\beta}(t,t')$ is a two-times function and instead of four we have 16 equations representing the evolution of the dot from any inital state α to any final state β. For every inital state there are four coupled equations of the form

$$K_{\alpha\beta}(t,t') = K^{(0)}_{\alpha\beta}(t,t') + \sum_{\gamma\delta}\int_0^t dt_1 \int_0^{t'} dt_2 K_{\alpha\gamma}(t_1,t_2)\mathbf{\Delta}_{\gamma\delta}(t_1,t_2)G^{\dagger}_{\delta\beta}(t-t_1)G_{\delta\beta}(t'-t_2).$$

The vertex functions without inter-branch hybridization lines are composed by the bold propagators on the upper and lower branch

$$K^{(0)}_{\alpha\beta}(t,t') = \delta_{\alpha\beta}G^{\dagger}_{\alpha\beta}(t)G_{\alpha\beta}(t').$$

The self consistent equations for the initially unoccupied dot are

$$K_{00}(t,t') = K^{(0)}_{00}(t,t') + \int_0^t dt_1 \int_0^{t'} dt_2 G^{\dagger}_0(t'-t_2)G_0(t-t_1)\Delta^{<}_{\uparrow}(t_1,t_2)K_{0\uparrow}(t_1,t_2) + \int_0^t dt_1 \int_0^{t'} dt_2 G^{\dagger}_0(t'-t_2)G_0(t-t_1)\Delta^{<}_{\downarrow}(t_1,t_2)K_{0\downarrow}(t_1,t_2)$$

$$K_{0\uparrow}(t,t') = \int_0^t dt_1 \int_0^{t'} dt_2 G^{\dagger}_{\uparrow}(t'-t_2)G_{\uparrow}(t-t_1)\Delta^{>}_{\uparrow}(t_1,t_2)K_{00}(t_1,t_2) + \int_0^t dt_1 \int_0^{t'} dt_2 G^{\dagger}_{\uparrow}(t'-t_2)G_{\uparrow}(t-t_1)\Delta^{<}_{\downarrow}(t_1,t_2)K_{0\uparrow\downarrow}(t_1,t_2)$$

$$K_{0\downarrow}(t,t') = \int_0^t dt_1 \int_0^{t'} dt_2 G^{\dagger}_{\downarrow}(t'-t_2)G_{\downarrow}(t-t_1)\Delta^{>}_{\downarrow}(t_1,t_2)K_{00}(t_1,t_2) + \int_0^t dt_1 \int_0^{t'} dt_2 G^{\dagger}_{\downarrow}(t'-t_2)G_{\downarrow}(t-t_1)\Delta^{<}_{\uparrow}(t_1,t_2)K_{0\uparrow\downarrow}(t_1,t_2)$$

$$K_{0\uparrow\downarrow}(t,t') = \int_0^t dt_1 \int_0^{t'} dt_2 G^{\dagger}_{\uparrow\downarrow}(t'-t_2) G_{\uparrow\downarrow}(t-t_1) \Delta^{>}_{\downarrow}(t_1,t_2) K_{0\uparrow}(t_1,t_2) + \int_0^t dt_1 \int_0^{t'} dt_2 G^{\dagger}_{\uparrow\downarrow}(t'-t_2) G_{\uparrow\downarrow}(t-t_1) \Delta^{>}_{\uparrow}(t_1,t_2) K_{0\downarrow}(t_1,t_2).$$

For equal times, $K_{\alpha\beta}(t,t)$ is the population probability on the dot. After initializing the vertex functions $K_{\alpha\beta}(t,t')$ with $K^{(0)}_{\alpha\beta}(t,t')$ and performing the self-consistent iteration sheme one is able to construct Greens functions in the following way

$$G^{>}_{\alpha\uparrow}(t,t') = -i\langle d_{\uparrow}(t) d^{\dagger}_{\uparrow}(t')\rangle = K_{\alpha 0}(t,t') * G_{\uparrow}(t-t') + K_{\alpha\downarrow}(t,t') * G_{\uparrow\downarrow}(t-t')$$

$$G^{<}_{\alpha\uparrow}(t,t') = i\langle d^{\dagger}_{\uparrow}(t') d_{\uparrow}(t)\rangle = K_{\alpha\uparrow}(t,t') * G_{0}(t-t') + K_{\alpha\uparrow\downarrow}(t,t') * G_{\downarrow}(t-t')$$

$$G^{>}_{\alpha\downarrow}(t,t') = -i\langle d_{\downarrow}(t) d^{\dagger}_{\downarrow}(t')\rangle = K_{\alpha 0}(t,t') * G_{\downarrow}(t-t') + K_{\alpha\uparrow}(t,t') * G_{\uparrow\downarrow}(t-t')$$

$$G^{<}_{\alpha\downarrow}(t,t') = i\langle d^{\dagger}_{\downarrow}(t') d_{\downarrow}(t)\rangle = K_{\alpha\downarrow}(t,t') * G_{0}(t-t') + K_{\alpha\uparrow\downarrow}(t,t') * G_{\uparrow}(t-t')$$

with α denoting the initial dot state. The conjugation yields to $\left(G^{>/<}(t,t')\right)^* = -G^{>/<}(t',t)$ and for particle-hole symmetric system $G^{>/<}(t,t') = -G^{>/<}(t',t)$. The advanced and retarded Green's function are defined via the lesser and greater component as

$$G^{R}(t,t') = -i\Theta(t-t')\langle \left[d(t), d^{\dagger}(t')\right]_{+}\rangle$$

$$G^{R}(t,t') = -i\Theta(t-t')\left(\langle d(t) d^{\dagger}(t')\rangle + \langle d^{\dagger}(t') d(t)\rangle\right)$$

$$G^{R}(t,t') = \Theta(t-t')\left(G^{>}(t,t') - G^{<}(t,t')\right)$$

and

$$G^{A}(t,t') = i\Theta(t'-t)\langle \left[d(t), d^{\dagger}(t')\right]_{+}\rangle$$

$$G^{A}(t,t') = i\Theta(t'-t)\left(\langle d(t) d^{\dagger}(t')\rangle + \langle d^{\dagger}(t') d(t)\rangle\right)$$

$$G^{A}(t,t') = -\Theta(t'-t)\left(G^{>}(t,t') - G^{<}(t,t')\right).$$

They have an intuitive interpretation since the imaginary part of their Fourier transforms gives the single particle spectral function

$$A(\omega) = -\frac{1}{\pi} \mathrm{Im} G^{R} = \frac{1}{\pi} \mathrm{Im} G^{A}.$$

4 Implementation

4.1 Bethe lattice

- Insert graphis of Bethe lattice structure and DOS

We will focus on the Hubbard model for a Bethe lattice in the limit of infinite dimensions, where DMFT becomes exact. With its semicircular Density of states

$$\mathrm{D}(\epsilon) = \frac{1}{2\pi \mathrm{v}_0^2}\sqrt{4\mathrm{v}_0 - \epsilon^2} \tag{5}$$

it relates the Greens function to the hybridization function in the simple way

$$\Delta(\omega) = \mathrm{v}_0^2 \mathrm{G}(\omega). \tag{6}$$

4.2 Initial state

The systems starts from in initial Néel state, which is a classical antiferromagnetic state

$$\mid \psi_{Neel} >= \prod_{i\epsilon A} d^\dagger_{i\uparrow} \prod_{j\epsilon B} d^\dagger_{j\downarrow} \mid 0 > .$$

It can be described by two identical sublattices with opposite magnetization, lattice A describing $\sigma =\uparrow$ and lattice B $\sigma =\downarrow$. It is sufficient to calculate the dynamics if only one sublattice since they obey the symmetry $G_{A,\sigma} = G_{B,-\sigma}$. The self-consistency condition for the Bethe lattice reads

$$\Delta_{A(B),\sigma}(t,t') = v(t) G_{B(A),\sigma}(t,t') v^*(t')$$

and using the symmetry it becomes

$$\Delta_\sigma(t,t') = v(t) G_{-\sigma}(t,t') v^*(t').$$

- Half filling
- Symmetries

4.3 Physical observables

- The observable we are interested in measures the energy that flows between the system and the heat bath and can be obtained from $I_E(t) = \langle \mathcal{I}_E(t) \rangle$. The energy current $\mathcal{I}_E(t)$ is defined as

$$\mathcal{I}_E = \dot{H}_{fBath} = i[H, H_{fBath}] + \frac{\partial H_{fBath}}{\partial t},$$

with $H = H_D + H_B + H_{hyb} + H_{fBath} + H_{fMix}$ describing the original Anderson impurity Hamiltonian 1. This leads to

$$\mathcal{I}_E = i[\sum_{k,\sigma}(V_k f^\dagger_{k,\sigma} d_\sigma + V_k^* d^\dagger_\sigma f_{k,\sigma}), \sum_{k',\sigma'} \varepsilon_{k'} f^\dagger_{k',\sigma'} f_{k',\sigma'}]$$

$$= i\sum_{k,\sigma}(V_k f^\dagger_{k,\sigma} d_\sigma + V_k^* d^\dagger_\sigma f_{k,\sigma})\varepsilon_k f^\dagger_{k,\sigma} f_{k,\sigma} - i\sum_{k,\sigma} \varepsilon_k f^\dagger_{k,\sigma} f_{k,\sigma}(V_k f^\dagger_{k,\sigma} d_\sigma + V_k^* d^\dagger_\sigma f_{k,\sigma})$$

$$= i \sum_{k,\sigma} \varepsilon_k (V_k d_\sigma f^\dagger_{k,\sigma} - V^*_k f_{k,\sigma} d^\dagger_\sigma)$$

- Energy current operator can be obtained by summing over all diagrams that have a special hybridization line that places the current operator at the tip of the Keldysh contour

$$I_E(t) = \int_0^t d\tau \Delta^<_f(t,\tau) G^<(t,\tau),$$

with the energy hybridization function $\Delta^<_f(t,\tau) = \int_{-\infty}^{\infty} \frac{d\omega}{\pi} exp^{-i\omega(t-\tau)} \omega \Gamma(\omega) f(\omega - \mu)$

- The system's response is measured by

$$P_{\omega_{probe}}(A_{probe}) = \lim_{A_{probe}\to 0} \frac{dI_E(A_{probe}(\omega_{probe}))}{dA_{probe}(\omega_{probe})} \simeq \frac{I_E(\Delta A_{probe}(\omega_{probe}))}{\Delta A_{probe}(\omega_{probe})}$$

and $A_{probe}(\omega_{probe})$ is the amplitude of the probe field3.3 with the probe frequency ω_{probe}.

4.4 Numerical implementation

Working with non-equilibrium systems involves explicit time dependence, so that all objects become two times functions. In order to solve the impurity problem, we need to solve Dyson equations of the form

$$\mathrm{G}_{\alpha\alpha}(\mathrm{t},\mathrm{t}') = \mathrm{G}^{(0)}_{\alpha\alpha}(\mathrm{t},\mathrm{t}') - \int_0^{\mathrm{t}} \mathrm{dt}_1 \int_0^{\mathrm{t}_1} \mathrm{dt}_2 \mathrm{G}^{(0)}_{\alpha\alpha}(\mathrm{t},\mathrm{t}_1) \Sigma_{\alpha\alpha}(\mathrm{t}_1,\mathrm{t}_2) \mathrm{G}_{\alpha\alpha}(\mathrm{t}_2,\mathrm{t}').$$

These are two-dimensional Volterra integral equations, which have a causal structure as the integral limits show. We compute every time-slice t by starting with $G_{\alpha\alpha}(t,t)$ and successively increasing t'.

5 Results

5.1 Equilibrium properties

- show how the DOS splits from non interacting case to high U

5.2 Magnetic relaxation in a periodically driven Hubbard model

Before exploring new physics, we want to reproduce well known phenomena. In their recent research Martin Eckstein and al. studied the melting of long-range antiferromagnetic order in a periodically driven repulsive Hubbard model. This chapter is orientated on their paper and reproduces part of the results. We are calculating the dynamics with non-equilibrium DMFT for a Bethe-lattice in infinite dimensions. First we investigate the melting in the absence of a driving field and in a second step we explore the effect of a strong driving field in the case of a resonant driving frequency. The two quantities we are focusing on are the double occupation $d(t) =< n_\uparrow(t) n_\downarrow(t) >$, which is measuring the formation of charge excitations and the magnetization $M(t) = \frac{<n_\uparrow(t) - n_\downarrow(t)>}{1-2d(t)}$ as an indicator for the antiferromagnetic order of the the system. The magnetization $M(t)$ is formed by the straggered magnetic order parameter, which is normalizes by the probability of a site being sinlgy occupied.

5.2.1 Undriven magnetic melting

To begin with, we will look at the melting mechanisms in different regimes in the undriven case ($A = 0$, $v = v_0 = 1$). In the Mott-insulating regime with a strong Coulomb interaction $U \gg v$, Fig. ? shows the magnetic order parameter $M(t)$ and the double occupation $d(t)$ for different values of U during the timeslice $0 \leq v_0 t \lesssim 6$. The dynamics of both entities start with oscillations at short times resulting from the Néel state not being an eigenstate of the Hubbard model at finite U and change their behavior after $v_0 t \simeq 1$. The formation of charge excitations relaxes fastly to a U dependent steady state value at a low rate since the strong Coulomb interaction is preventing electrons to hop across the lattice and the magnetization $M(t)$ shows a linear decrease with a U dependent gradient. The fast relaxation of the charge dynamics compared to the magnetization indicates that the magnetic melting is due to the movement of the charge excitations on top of the anti-ferromagnetic spin background. To further underpin this statement Eckstein and al. investigated the spin precession dynamics by flipping an initially located fermion at a single probe site in the x direction. An effective magnetic field B_{eff}, which is formed by the neighbouring sites, is orientated along the z direction leading to harmonic precession of the magnetic moment in the x-y plane. It turns out that the precessing magnetic moment sustains, even for times $v_0 t > 1$, which confirms that the decay of the magnetic order is due to mobile charge excitations and local magnetic moments are preserved.

When the Coulomb interaction is lowered, coming close to the non-interacting limit $U = 0$, one expects quasiparticles to be responsible for the dynamics of the system. For $U \lesssim 1$ the magnetization shows an oscillatory behaviour and decays to zero fastly, while $d(t)$ relaxes to high values (Fig. ?). Compared to the results for $U \gg v$, where the spin dynamics relax much slower than the charge dynamics, here $M(t)$ and $d(t)$ both relax around $v_0 t \simeq 1$, indicating that the destruction of the anti ferromagnetic order is caused by the destruction of local magnetic moments.

TODO: figures comparing my results with Martin's, explain that our result coincide better for high vlaues of U.

Figure 1: Dynamics of our system without driving for high Coulomb interactions. Top: Decay of magnetic order parameter $M(t)$. Bottom: Decay of double occupation $d(t)$. Zoom into short time dynamics, because we refer to it in the text.

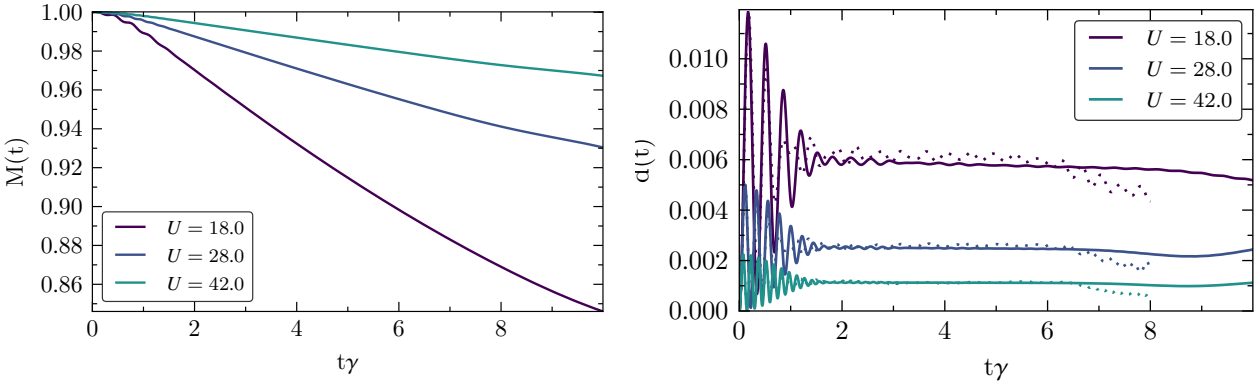

- Explain why d(t) becomes unstable after t=8

5.2.2 Magnetic melting in resonant driven lattices

- Martin Eckstein and al are exploring the effects of a driving field in three different regimes: high frequency, resonant and in gap away from resonant driving; we will focus only on the case of resonant driving.
- Resonant driving modifies the behaviour of $M(t)$ and $d(t)$ strongly; the magnetization changes from a slow decay in the absence of driving to a fast decay even for small driving amplitudes and the double occupation goes from a saturation at low values to high values resembling the case for $U \lesssim 1$; it is a tool to switch from the charge-excitation to the quasiparticle melting mechanism and control the relaxation speed of the charge and spin dynamics.
- explain attractive interaction

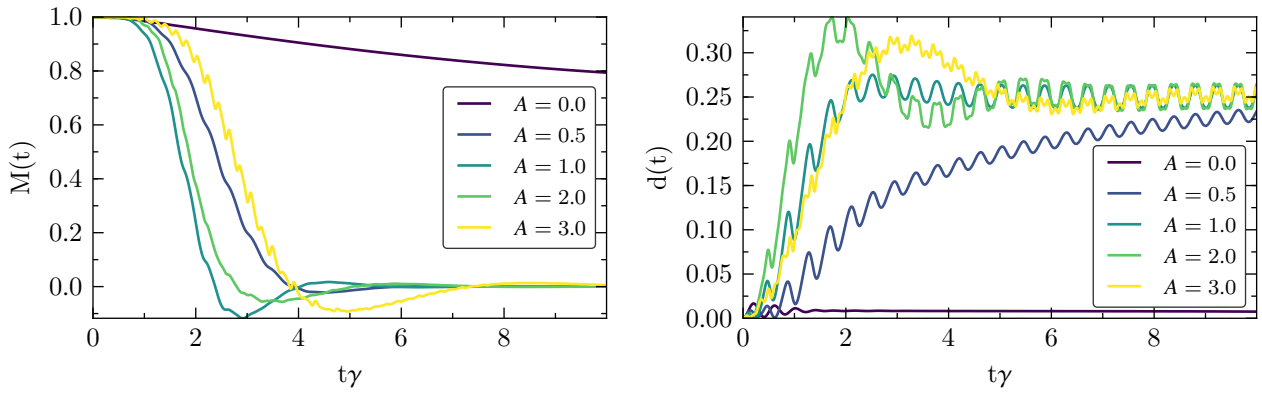

Figure 2: Dynamics of our system with $U = \omega = 15$ and various amplitudes. Left: Decay of magnetic order parameter $M(t)$. Right: Decay of double occupation $d(t)$.

5.3 Pump-Probe Experiements

- We want to investigate how the system's response to a small pertubation changes when it is driven out of equilibrium.
- The response of the system is the derivative $P_{\omega_{probe}}$ of the energy current with respect to the probe amplitude. For a pump field with the pump amplitude A_{pump} and pump frequency ω_{pump} it is obtained by

$$P_{\omega_{probe}} \simeq \frac{I_E(\Delta A_{probe}(\omega_{probe}))}{\Delta A_{probe}(\omega_{probe})} = \frac{I_E(A_{probe}(\omega_{probe})) - I_E(A_{probe=0}(\omega_{probe}))}{A_{probe}(\omega_{probe}) - A_{probe=0}(\omega_{probe})}$$

- An example of the energy current5.3 at resonant driving shows that a steady state emerges after $v_0 t \simeq 3$. We are taking the average value of $P_{\omega_{probe}}$ over a period T to estimate the amout of energy that is flowing into the heat bath, which we will name $\bar{P}_{\omega_{probe}}$. The errorbars are calculated from the difference of $\overline{P}_{\omega_{probe}}$ between two periods.

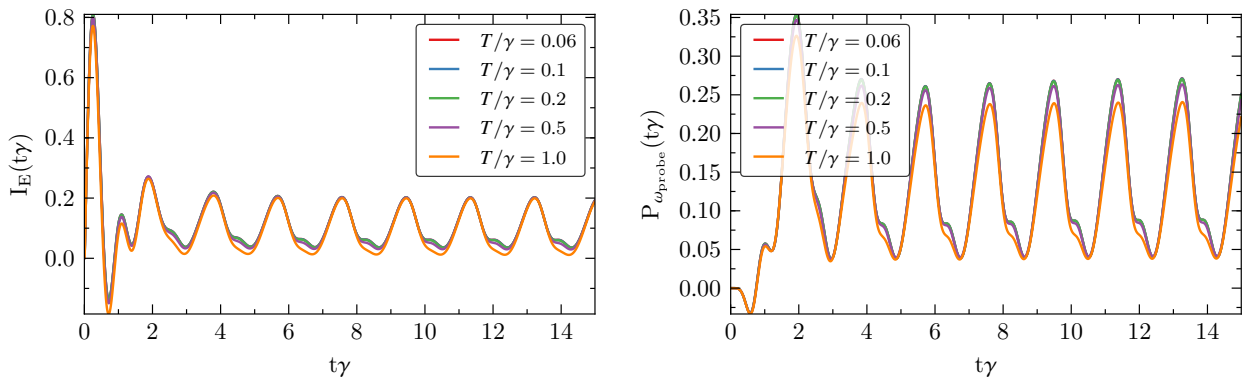

Figure 3: Left: Heat current for $A_{pump} = 1.0, \omega_{pump} = \omega_{probe} = 5$ and $A_{probe} = 0.1$. Right: Relative current for the same parameters

5.3.1 Resonant Pumping

We start discussing results for a Coulomb interaction of $U = 5$ while the system is exposed to an electric field with the frequency of the bandgap and various amplitudes. During the whole simulation energy can dissipate into a fermion bath, with a flat desity of states as described in 3.4 and the coupling strength $\lambda = 0.5$. Going to a finite U after the system was initially in a zero-temperature anti-ferromagnetic state with $U \to \infty$ corresponds to a strong quench in the Coulomb interaction. The external bath functions not only as a dissipation mechanism so that a steady state can emerge, it also fixes the temperature of the system.

Looking at the spectral function without driving 5.3.1 shows an upper and lower Hubbard band for high temperatures and the formation of low frequency excitations for $T \leq 0.2$, an indicator for Kondo physics. We can estimate the Kondo temperature over the formula $k_B T_K = U\sqrt{\frac{\Gamma}{2U}} \exp^{-\frac{\pi U}{8\Gamma} + \frac{\pi\Gamma}{2U}}$, which results in $k_B T_K = 0.16$. Increasing the amplitude of the driving field effectively increases the temperature and therefore leads to the destruction of the Kondo peak. A resonant driving field pumps electrons/holes between the lower/upper Hubbard band and accelerates the equilibration of the system, for $A = 1.0$ the spectral functions are all symmetric and temperature independent except the leftovers of a small Kondo peak.

Probing at a frequency corresponding to the energy difference between th side bands and the Kondo peak ($\omega_{probe} = 2.5$) shows a small response for $A = 0$ and goes to negative values for $A \geq 0.5$, which can be interpreted as an energy flow from the bath into the system. Probing at the same frequency as we are pumping shows that the response first increases as we would expect from the evolution of the spectral functions 5.3.1. This trend changes at the treshold value of $A = 1.0$ and the response starts to decrease again until the response of the highest pump amplitude reaches the same scale as the response without a driving field.

It is also surprising that there is almost no temperature dependance seen in the response functions, especially for small pump amplitudes. Obviously the response carries information, which is not contained in the single-particle Greens functions we are calculating.

- spin averaged and time evolved spectral functions
- TODO: Add dynamics of M and d to compare the different melting mechanisms

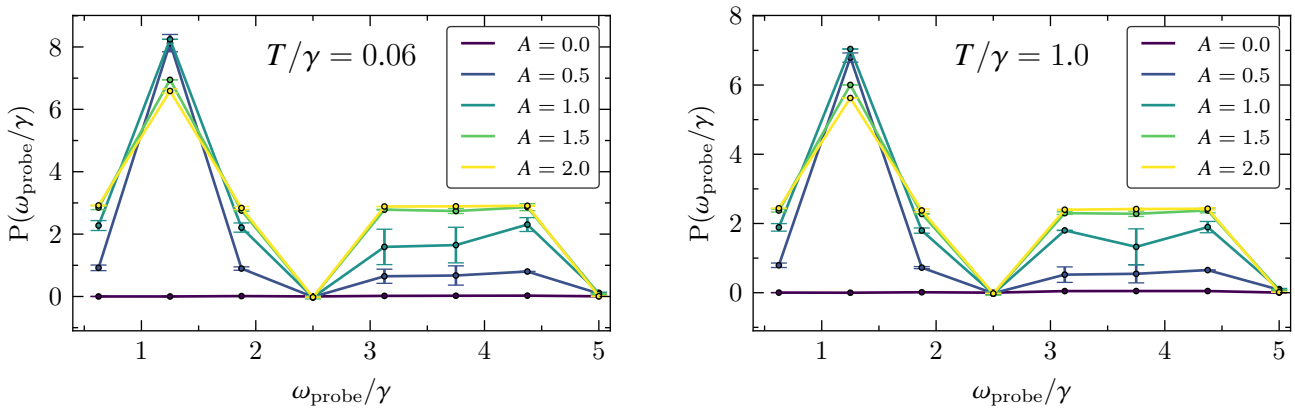

Figure 4: Linear response at resonant pumping for temperatures $T/\gamma = 0.06$ and $T/\gamma = 1.0$

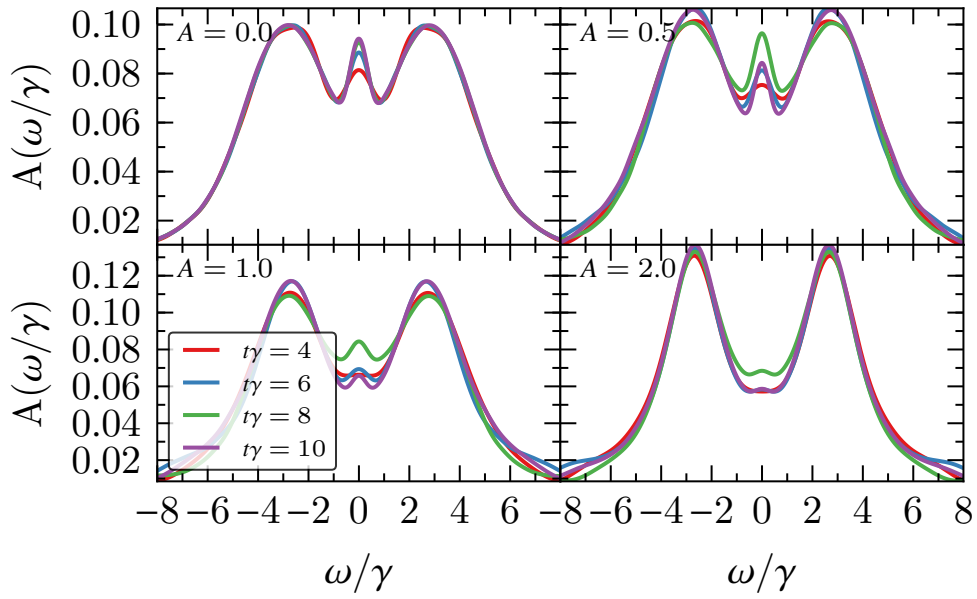

Figure 5: Time-evolved spectral functions, averaged over the initial spin-up and spin-down state at different temperatures. A resonant electric field ($\omega_{pump} = 5$) with increasing strength is applied.

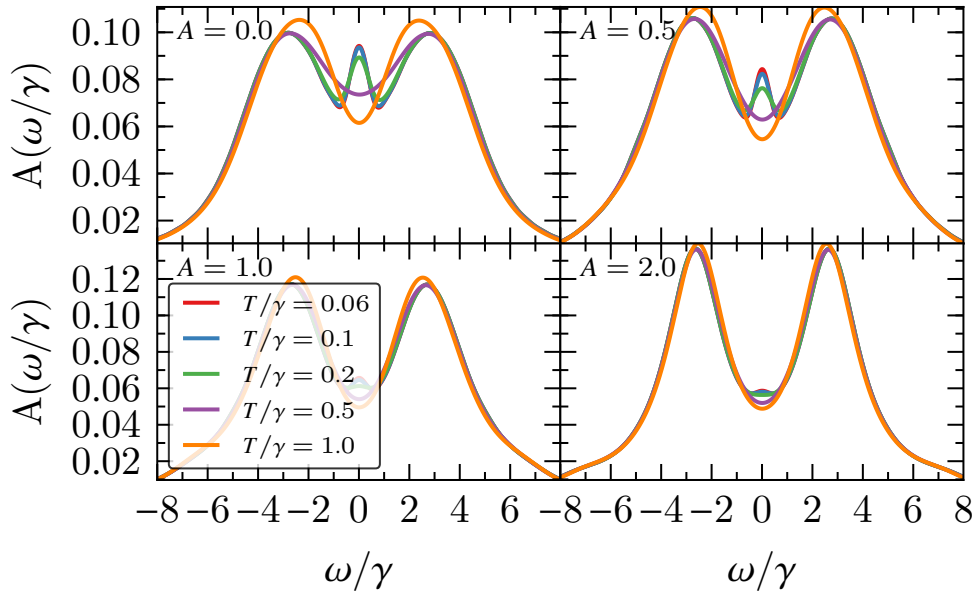

Figure 6: Spectral function averaged over an initial spin up and spin down dot state for different temperatures and various pump amplitudes at resonant driving.

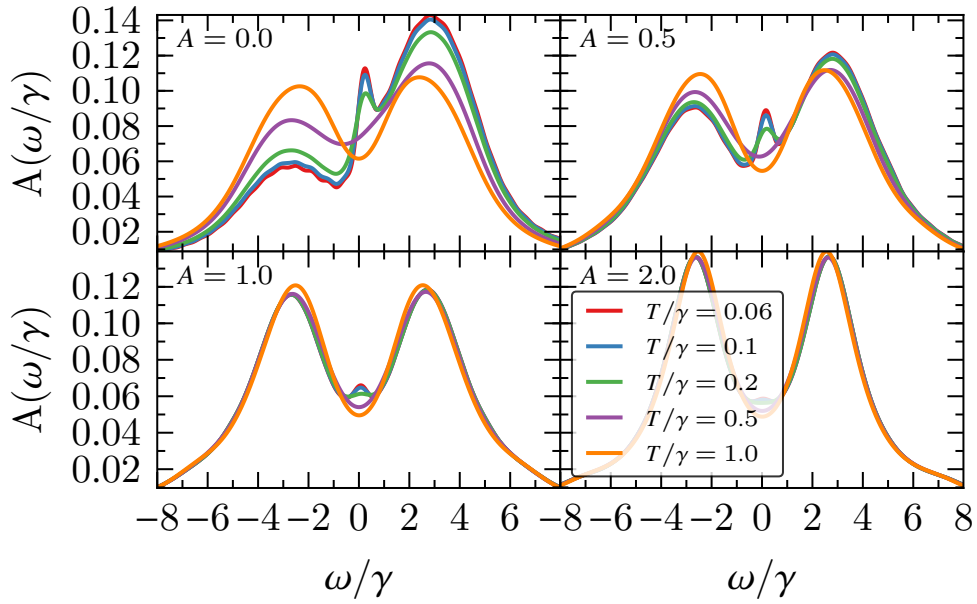

Figure 7: Spectral functions for an initial spin-up state for different temperatures and pump amplitudes at resonant driving.

5.4 Half-Resonant Pumping

We are doing the same analyzation for a pump frequency of half the bandgap.

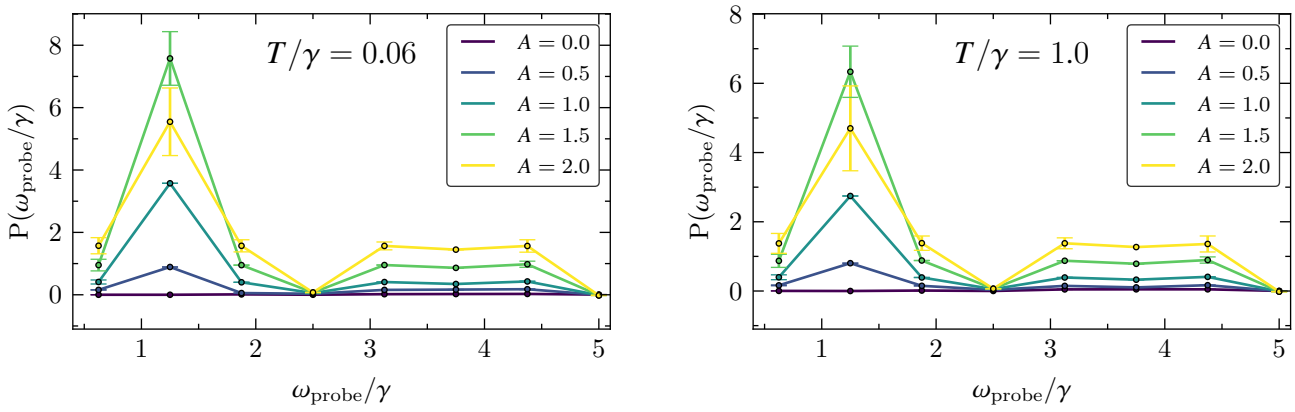

Figure 8: Linear response at half-resonant pumping for temperatures $T/\gamma = 0.06$ and $T/\gamma = 1.0$

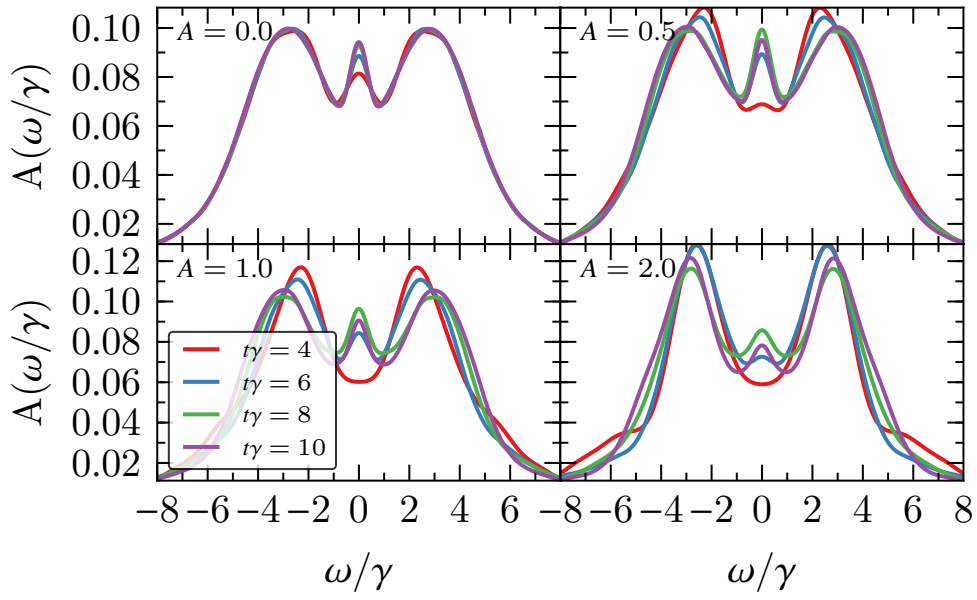

Figure 9: Time-evolved spectral functions, averaged over the initial spin-up and spin-down state at different temperatures. A half-resonant electric field ($\omega_{pump} = 2.5$) with increasing strength is applied.

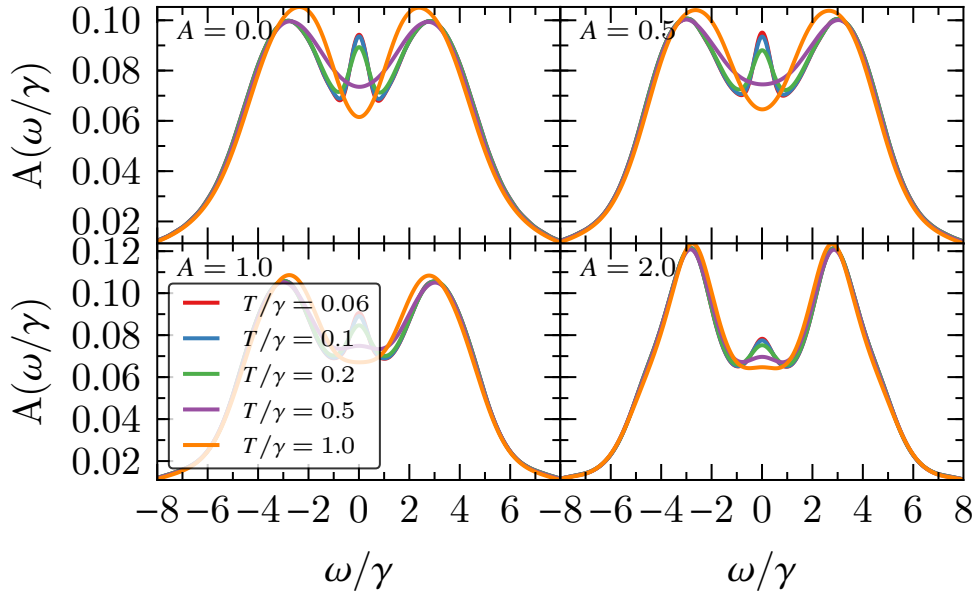

Figure 10: Spectral function averaged over an initial spin up and spin down dot state for different temperatures and various pump amplitudes at half-resonant driving.

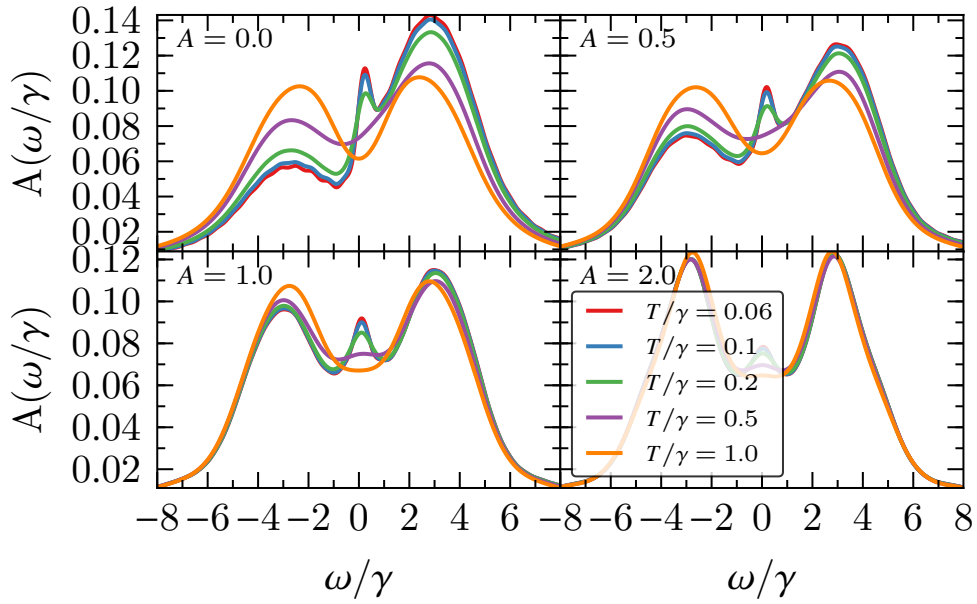

Figure 11: Spectral functions for an initial spin-up state for different temperatures and pump amplitudes at half-resonant driving.

5.5 Decoupling from the dissipation bath

5.5.1 Resonant driving

- without coupling

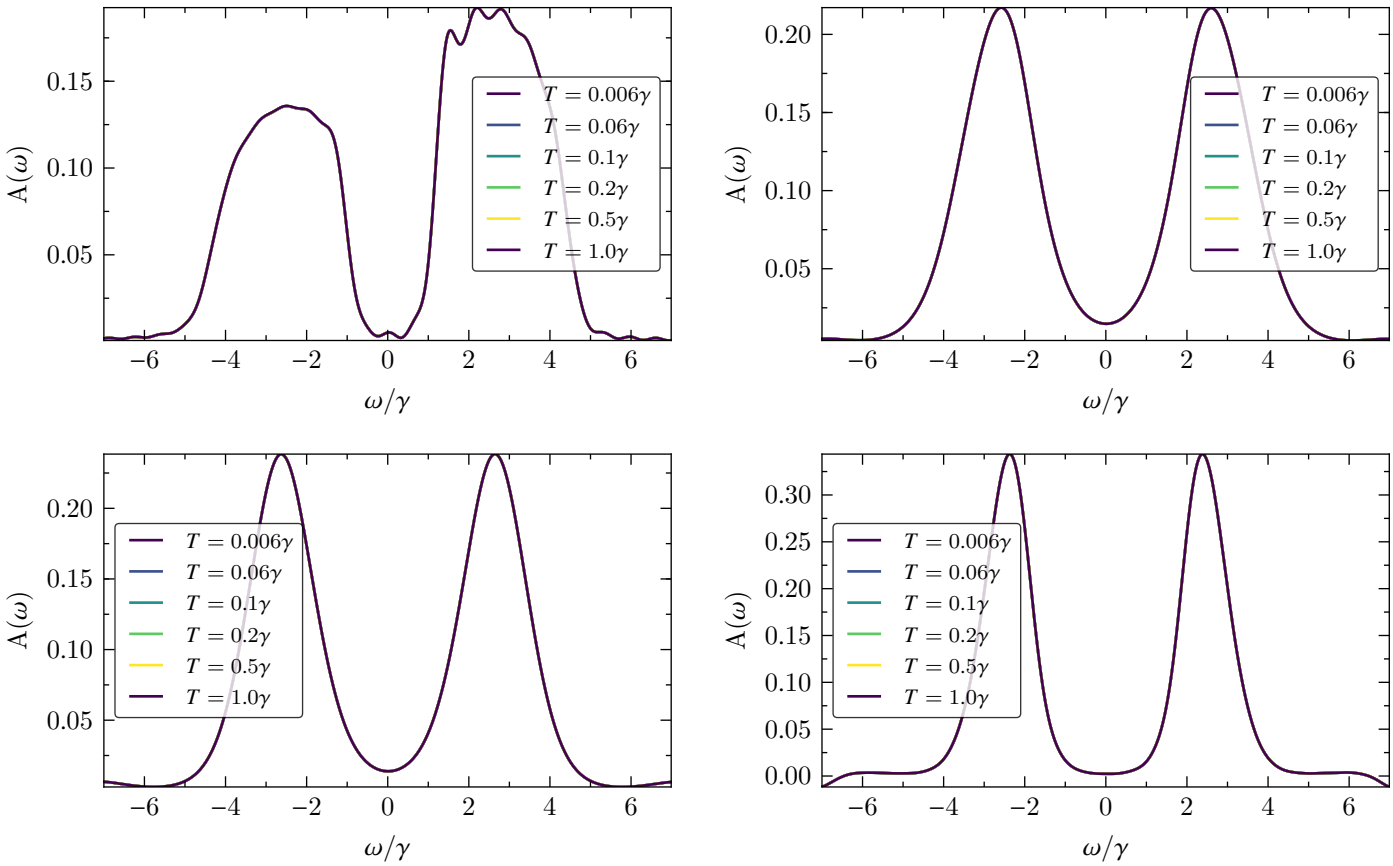

Figure 12: Spectral function for different temperatures at resonant driving ($\omega_{pump} = 5$) without a dissipation mechanism. Top left: without driving ($A_{pump} = 0.0$); top right: $A_{pump} = 0.5$; bottom left: $A_{pump} = 1.0$; Bottom right: $A_{pump} = 2.0$

- decoupling at $t \gtrsim 2$

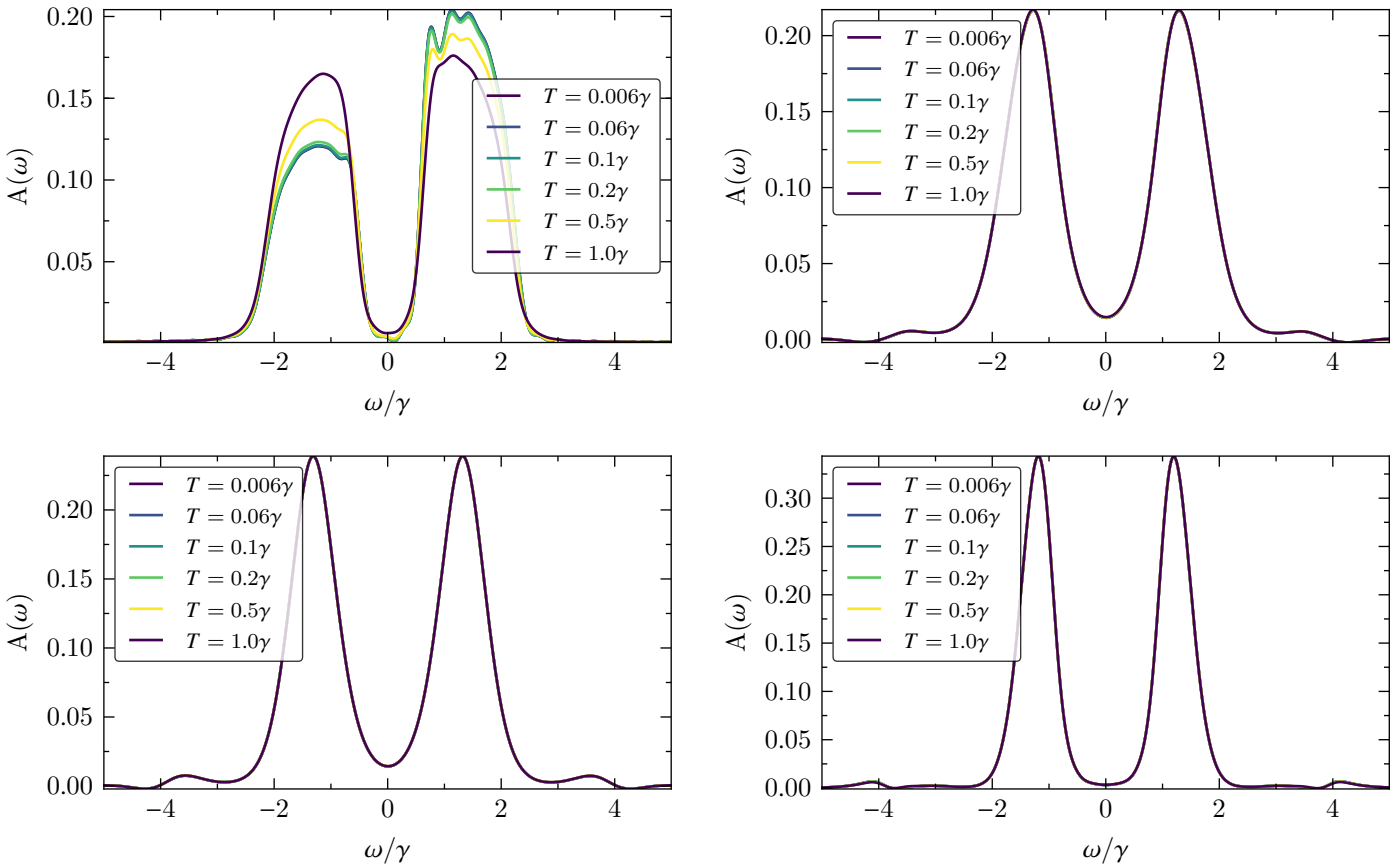

Figure 13: Spectral function for different temperatures at resonant driving ($\omega_{pump} = 5$) while the system is decoupled from the bath at $t \gtrsim 2$. Top left: without driving ($A_{pump} = 0.0$); top right: $A_{pump} = 0.5$; bottom left: $A_{pump} = 1.0$; Bottom right: $A_{pump} = 2.0$

- decoupling at $t \gtrsim 4$

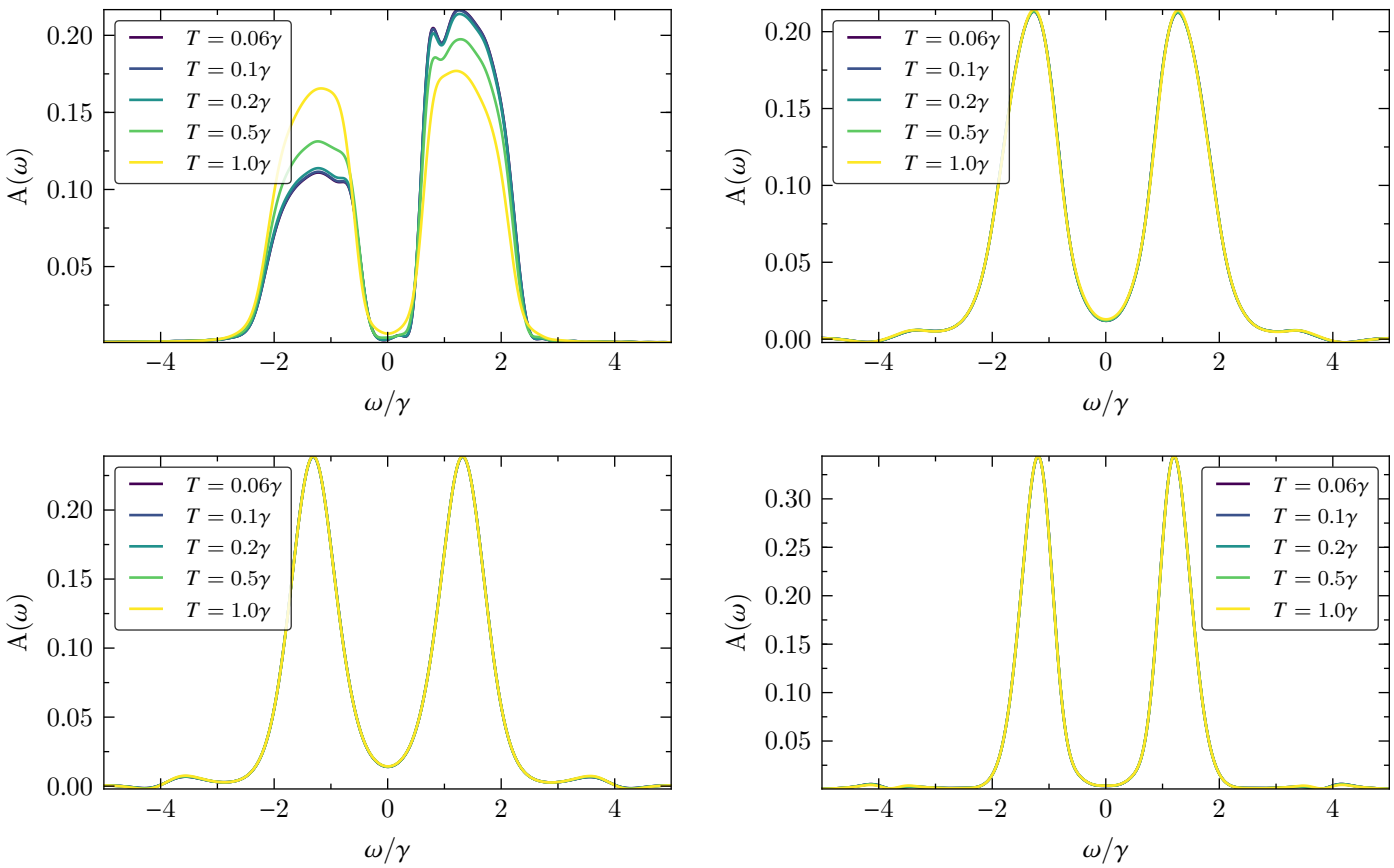

Figure 14: Spectral function for different temperatures at resonant driving ($\omega_{pump} = 5$) while the system is decoupled from the bath at 4. Top left: without driving ($A_{pump} = 0.0$); top right: $A_{pump} = 0.5$; bottom left: $A_{pump} = 1.0$; Bottom right: $A_{pump} = 2.0$

5.5.2 Half-resonant driving

- without coupling

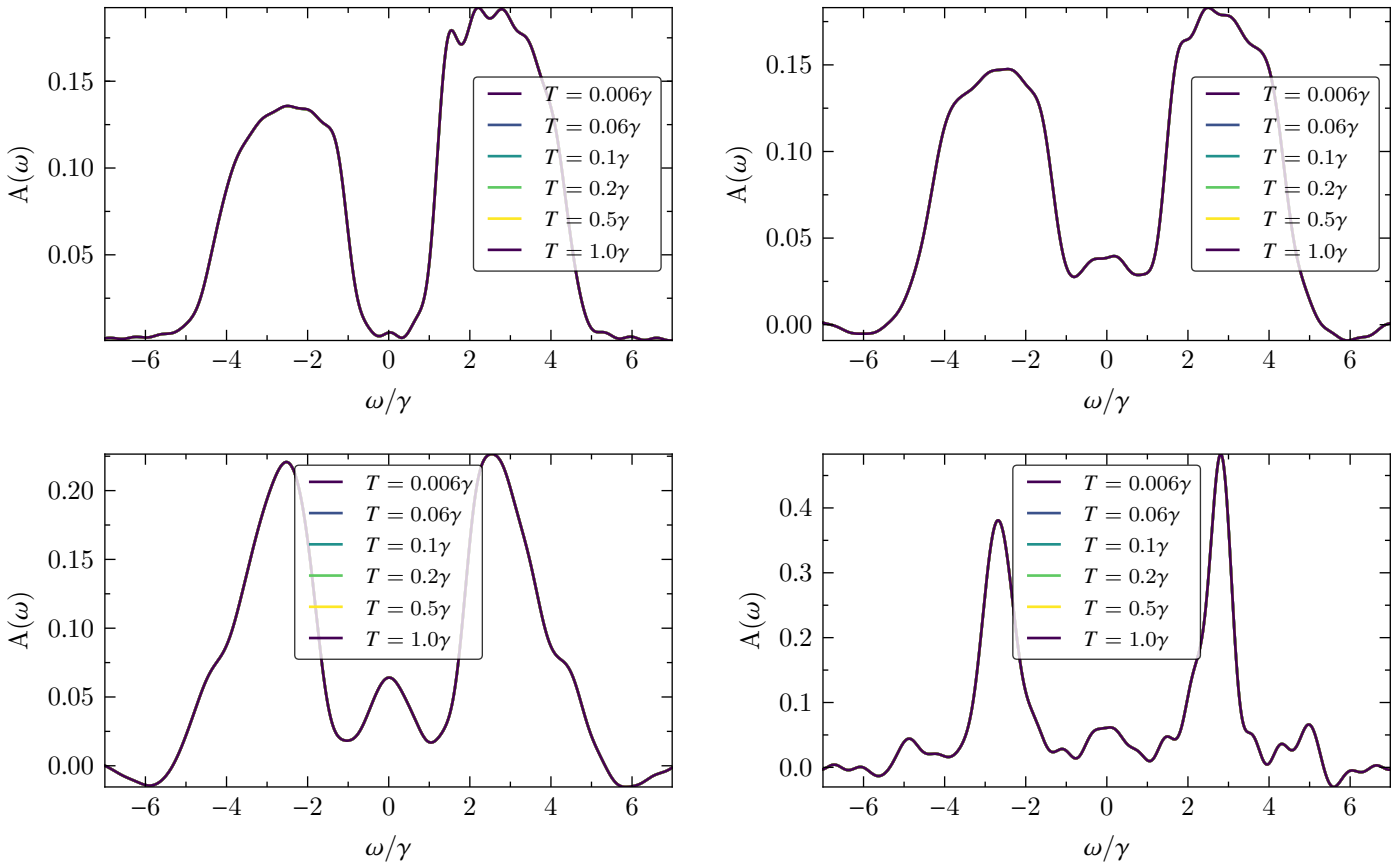

Figure 15: Spectral function for different temperatures at resonant driving ($\omega_{pump} = 5$) without a dissipation mechanism. Top left: without driving ($A_{pump} = 0.0$); top right: $A_{pump} = 0.5$; bottom left: $A_{pump} = 1.0$; Bottom right: $A_{pump} = 2.0$

- decoupling at $t \gtrsim 2$

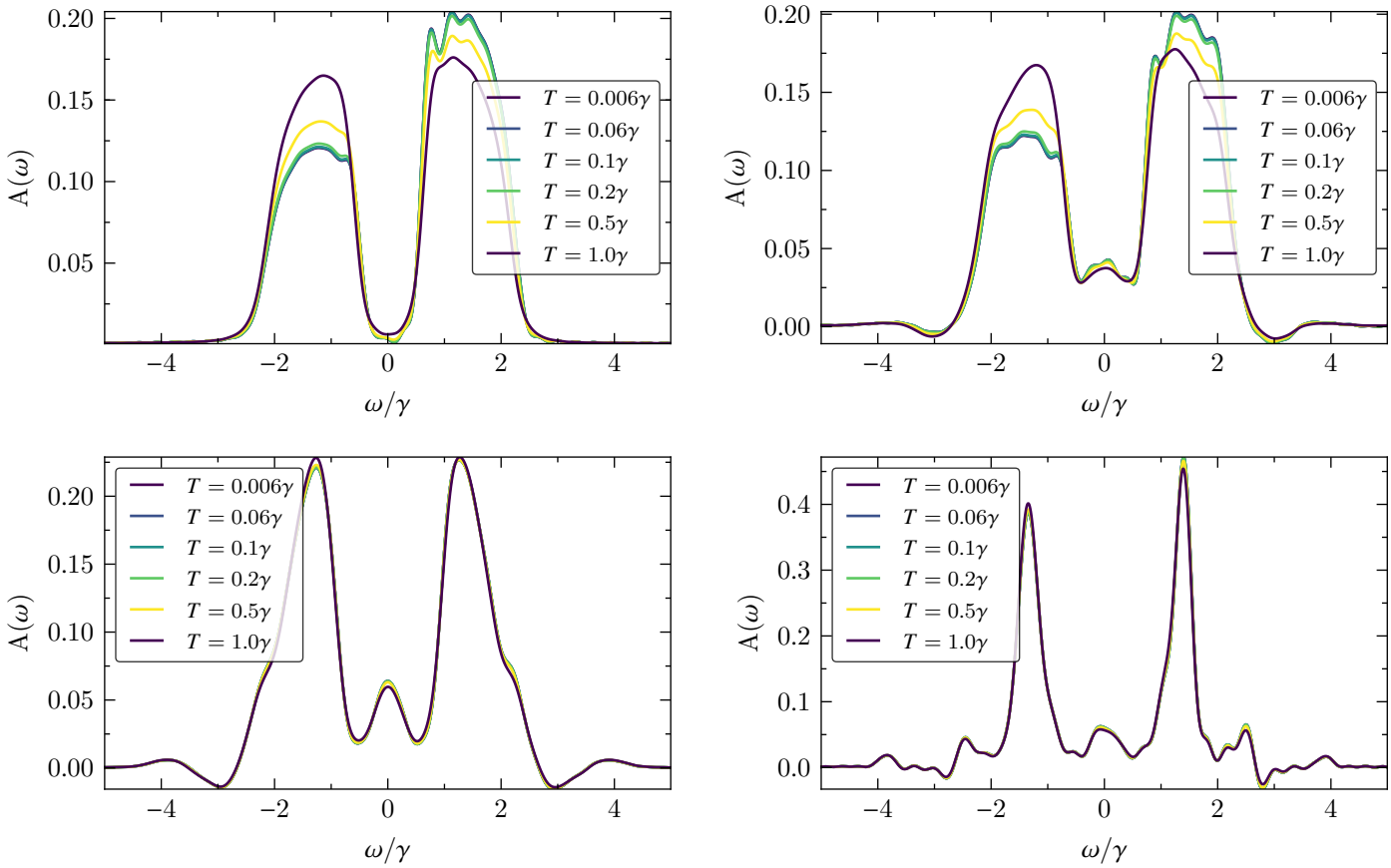

Figure 16: Spectral function for different temperatures at resonant driving ($\omega_{pump} = 5$) while the system is decoupled from the bath at $t \gtrsim 2$. Top left: without driving ($A_{pump} = 0.0$); top right: $A_{pump} = 0.5$; bottom left: $A_{pump} = 1.0$; Bottom right: $A_{pump} = 2.0$

- decoupling at $t \gtrsim 4$

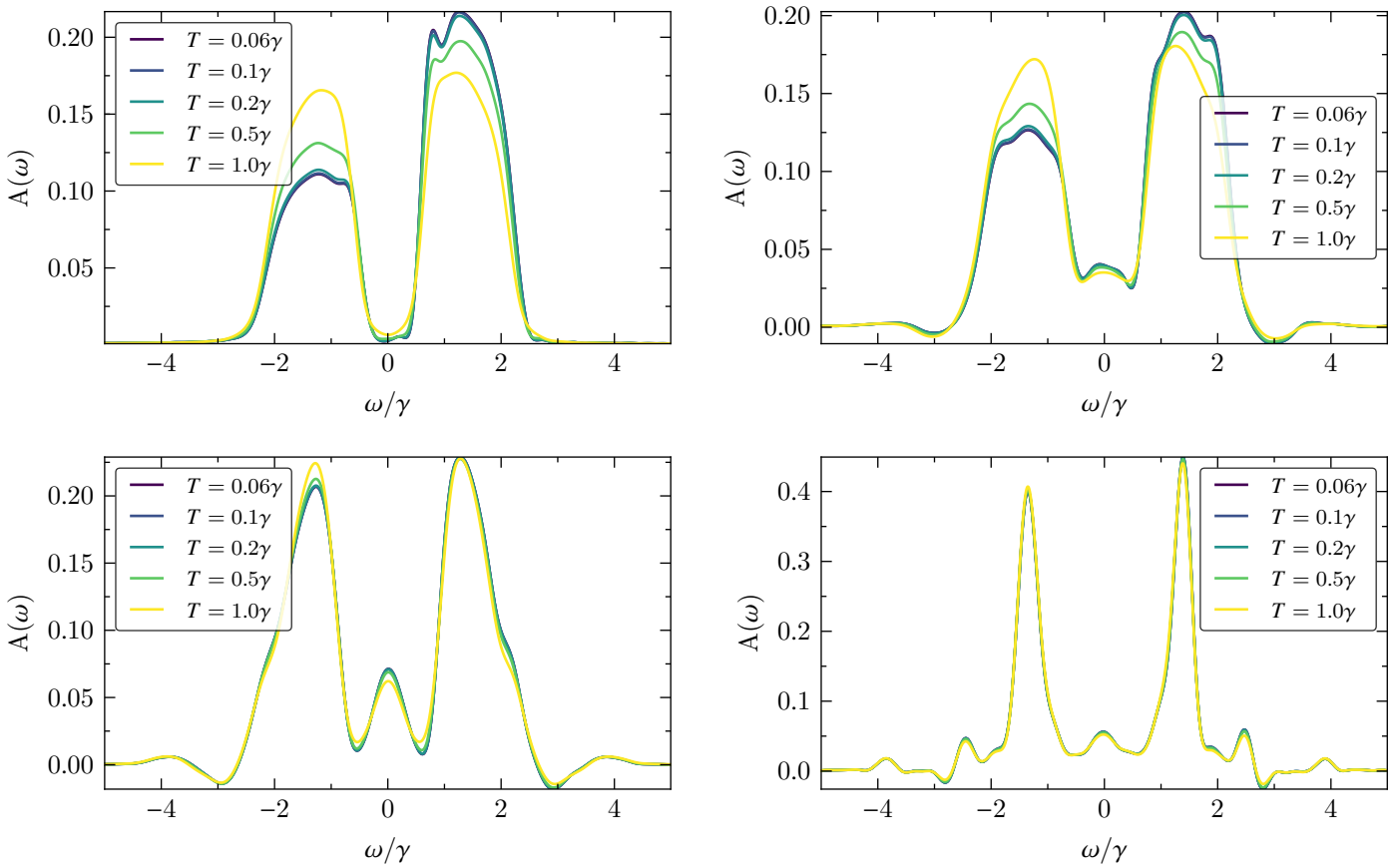

Figure 17: Spectral function for different temperatures at resonant driving ($\omega_{pump} = 5$) while the system is decoupled from the bath at 4. Top left: without driving ($A_{pump} = 0.0$); top right: $A_{pump} = 0.5$; bottom left: $A_{pump} = 1.0$; Bottom right: $A_{pump} = 2.0$

6 Conclusion